

Electrical Double Layer in Imidazolium Chloroaluminate Ionic Liquids and Its Influence on the Surface Morphology of Aluminium Deposits

Yong Zheng^{1,*}, Yongjun Zheng¹, Conghu Peng¹, Zhijun Zhao², Dayong Tian¹

¹College of Chemistry and Environmental Engineering, Anyang Institute of Technology, Anyang 455000, Henan, P. R. China

²State Key Laboratory of Chemical Engineering, Department of Chemical Engineering, Tsinghua University, Beijing 100084, P. R. China

*E-mail: yzheng83@126.com

Received: 21 June 2016/ Accepted: 27 August 2016 / Published: 10 October 2016

The traditional electrolytic process in aluminium industry suffers from many inherent problems, which are mainly owing to the natural drawbacks of electrolytes. The development of ionic liquid provides a promising approach for low-temperature aluminium electrodeposition. Although extensive research has been reported, the relationship between ionic liquids' structure and electrodeposition process is still little understood. To investigate this fundamental issue, some typical imidazolium chloroaluminate ionic liquids were synthesized and investigated as electrolytes in this work. Experimental results show that the structure of cation has significant effect on surface morphology of aluminium deposits. This fact results from the different structure of electrical double layer at electrode interface. Based on theoretical calculations, it's first found that aluminium is harder to be electrodeposited and the average grain size of deposits becomes larger with increasing cation-anion interaction energy. In such case, $[\text{Al}_2\text{Cl}_7]^-$ anion cannot easily penetrate double layer and be adsorbed onto the electrode, which always results in larger aluminium crystals. Furthermore, the value of interaction energy is proved to be highly affected by the structure of *N*-alkyl side chain, especially functional group. Therefore, interaction energy should be adjusted to a lower value by regulating the structure of imidazolium cation, in order to achieve finer and smoother aluminium crystals from chloroaluminate ionic liquids. It's expected that present work will help to promote the future research in this important field.

Keywords: electrical double layer; aluminium; morphology; chloroaluminate ionic liquids

1. INTRODUCTION

Aluminium has been widely used over the world owing to its attractive physicochemical properties. As is well known, aluminium industry mainly includes the electrolysis, electrorefining and

electroplating of aluminium. Nowadays, the electrolysis and electrorefining processes are generally conducted in molten inorganic salts over the melting point of aluminium [1]. However, these methods have some inherent disadvantages, such as massive emission of carbon dioxide and perfluorocarbon, high operating temperature and energy consumption [2]. On the other hand, the organic systems used in aluminium electroplating are unsafe due to their volatility, flammability and low chemical stability [3]. Therefore, it's necessary to develop more efficient and environmental-friendly electrolytes.

Ionic liquids (ILs) have gained considerable interest as green media in a wide range of research since the 1990s [4]. Especially in electrochemical reactions, ILs exhibit more favorable properties over traditional electrolytes, such as high electrical conductivity, broad electrochemical windows, negligible vapor pressure and non-flammability [5,6]. Therefore, the development of ILs provides an innovative approach to aluminium electrodeposition at low temperature (<100°C). Compared with molten inorganic salts and organic solvents, lower energy consumption, improved current efficiency and higher quality of aluminium can be achieved by electrolysis in ILs [7].

Until now, most of published literature mainly focuses on the electrodeposition of aluminium from Lewis acidic chloroaluminate ILs. In these acidic systems, $[\text{Al}_2\text{Cl}_7]^-$ anion is electroactive and responsible for aluminium deposition, which results from the combination of organic chloride salts with a molar excess of anhydrous aluminium chloride [8,9]. Over the past few years, it has also been found that nano- and microcrystalline aluminium could be obtained from imidazolium chloroaluminate ILs [10-12]. The tunable structure and physicochemical properties of ILs make it easier to achieve various aluminium deposits. Therefore, it gives access to the revolution of aluminium industry in electroplating, nanocrystalline and functional material production.

Undoubtedly, the electrodeposition mechanism and surface morphology of aluminium are fundamental issues that are critical to relevant research. It should be noted that the electrodeposition process highly depends on charge and mass transfer across electrode/ILs interface. The corresponding electrical double layer formed between ions and electrode has significant influence on the electrochemical reaction mechanism and growth behavior of aluminium [13-15]. Although some studies have been carried out on electrical double layer, the understanding of relationship between its structure in chloroaluminate ILs and surface morphology of aluminium is very limited. From the perspective of scientific theory and industrial application, more efforts will be devoted to studying the role of double layer in aluminium deposition.

Motivated by this research background, we aimed to make a deep investigation of electrical double layer and its influence on the surface morphology of aluminium in chloroaluminate ILs. In view of excellent properties and performance in aluminium electrodeposition, some typical Lewis acidic methylimidazolium chloroaluminate ILs with different *N*-alkyl side chains were synthesized and characterized, which includes 1-hydrogen-3-methylimidazolium chloroaluminate ($[\text{H}_1\text{mim}]\text{Cl}/\text{AlCl}_3$), 1-ethyl-3-methylimidazolium chloroaluminate ($[\text{Emim}]\text{Cl}/\text{AlCl}_3$), 1-allyl-3-methylimidazolium chloroaluminate ($[\text{Amim}]\text{Cl}/\text{AlCl}_3$), 1-butyl-3-methylimidazolium chloroaluminate ($[\text{Bmim}]\text{Cl}/\text{AlCl}_3$) and 1-hexyl-3-methylimidazolium chloroaluminate ($[\text{Hmim}]\text{Cl}/\text{AlCl}_3$). On this basis, the surface morphology of aluminium deposits obtained from these ILs has been compared and analyzed. To probe into the relationship between electrodeposition process and electrical double layer at the electrode/ions interface, systemic electrochemical measurements and density functional theory

calculations were both carried out. According to the experimental results, the structure and formation process of double layer was discussed in detail. It first reveals the profound influence of cation-anion interaction energy on the electrodeposition behavior and morphology of aluminium. In addition, the method for regulating aluminium deposits through ILs' structure has also been proposed.

2.EXPERIMENTAL

2.1.Reagents

Most of the chemicals used in this work were purchased commercially from Alfa Aesar and Sinopharm Chemical Reagent Co., Ltd. *N*-Methylimidazolium (analytic grade, mass fraction purity >99.5%), 1-chlorobutane (analytic grade, mass fraction purity >99.5%), acetone (analytic grade, mass fraction purity >99.5%), allyl chloride (analytic grade, mass fraction purity >99.5%), ethyl acetate (analytic grade, mass fraction purity >99.5%), acetonitrile (analytic grade, mass fraction purity >99.5%) and absolute alcohol (analytic grade, mass fraction purity >99.5%) were purified by distillation. Anhydrous aluminium chloride (analytic grade, mass fraction purity >99%), silver nitrate (analytic grade, mass fraction purity >99.8%), hydrochloric acid (analytic grade, HCl mass fraction purity 36~38%) and sulfuric acid (analytic grade, H₂SO₄ mass fraction purity >98%) were used without further purification. 1-Ethyl-3-methylimidazolium chloride ([Emim]Cl) (analytic grade, mass fraction purity >99.5%), 1-hexyl-3-methylimidazolium chloride ([Hmim]Cl) (analytic grade, mass fraction purity >99.5%) and 1-butyl-3-methylimidazolium bis(trifluoromethylsulfonyl)imide ([Bmim][NTf₂]) (analytic grade, mass fraction purity >99.5%) were obtained from Tokyo Chemical Industry Co., Ltd and Linzhou Keneng Material Technology Co., Ltd.

2.2. Synthesis and characterization of ILs

1-Hydrogen-3-methylimidazolium chloride ([H₁mim]Cl). According to Ohno et al.'s work [16], 1.1 mole of hydrochloric acid was added drop-wise into 1 mole of *N*-methylimidazolium under stirring at 273 K. Then, the mixture was heated up to 333 K and stirred for another 6 h. After the resulting solution was concentrated by rotary evaporation, the residual liquid was extracted by acetone and dried under vacuum at 343 K for 48 h. The IL was finally obtained as colorless solid at room temperature. ¹H NMR: δ = 12.402 (s, 1H), 9.286 (s, 1H), 7.793 (d, 1H), 7.691 (d, 1H), and 3.927 (s, 3H) ppm [17].

1-Allyl-3-methylimidazolium chloride ([Amim]Cl). This IL was synthesized according to method described in the literature [18]. The final IL was obtained as a pale yellow liquid at room temperature. ¹H NMR (DMSO-*d*₆): δ = 9.434 (s, 1H), 7.786 (d, 1H), 7.769 (d, 1H), 6.005 (m, 1H), 5.282 (m, 2H), 4.865 (d, 2H) and 3.853 (s, 3H) ppm [18].

1-Butyl-3-methylimidazolium chloride ([Bmim]Cl). As Huddleston et al. described [19], 1 mole of *N*-methylimidazolium and 1.15 mole of 1-chlorobutane were added to a flask and stirred at 343 K for 48 h. Then, the mixture was washed by ether acetate, recrystallized from acetone and dried under vacuum. The final IL was obtained as white wax-like solid at room temperature. ¹H NMR

(DMSO- d_6): $\delta = 9.446$ (s, 1H), 7.840 (d, 1H), 7.765 (d, 1H), 4.177 (t, 2H), 3.856 (s, 3H), 1.747 (m, 2H), 1.233 (m, 2H), and 0.873 (m, 3H) ppm [20].

Lewis acidic imidazolium chloroaluminate ILs ([Rmim]Cl/AlCl₃). The synthesis and following purification processes were all conducted under the dry argon atmosphere in a glove box (Universal, Mikrouna Co.), in which the content of oxygen and water was both kept below 1 ppm [20]. Lewis acidic imidazolium chloroaluminate ILs were prepared by mixing precise molar quantities of the corresponding imidazolium chloride salts with excess anhydrous aluminium chloride at room temperature. The resulting liquids have been filtered through glass frit and purified by electrolysis method before use. The final products were obtained as colorless liquids at room temperature. ¹H NMR of 1:2 [H₁mim]Cl/AlCl₃: $\delta = 10.102$ (s, 1H), 8.099 (s, 1H), 7.108 (d, 1H), 7.025 (d, 1H), 3.618 (s, 3H) ppm. ¹H NMR of 1:2 [Emim]Cl/AlCl₃: $\delta = 8.076$ (s, 1H), 7.157 (s, 1H), 7.118 (d, 1H), 4.031 (m, 2H), 3.725 (s, 3H), 1.350 (t, 3H) ppm. ¹H NMR of 1:2 [Amim]Cl/AlCl₃: $\delta = 7.954$ (s, 1H), 7.016 (d, 1H), 7.002 (d, 1H), 5.691 (m, 1H), 5.183 (m, 2H), 4.446 (d, 2H), 3.602 (s, 3H) ppm. ¹H NMR of 1:2 [Bmim]Cl/AlCl₃: $\delta = 7.931$ (s, 1H), 6.997 (d, 1H), 6.969 (d, 1H), 3.858 (t, 2H), 3.610 (s, 3H), 1.599 (m, 2H), 1.118 (m, 2H), 0.697 (m, 3H) ppm [20]. ¹H NMR of 1:2 [Hmim]Cl/AlCl₃: $\delta = 7.680$ (s, 1H), 6.731 (s, 1H), 6.705 (d, 1H), 3.564 (t, 2H), 3.322 (s, 3H), 1.294 (m, 2H), 0.703 (m, 6H), 0.241 (t, 3H) ppm.

The NMR measurements of ILs were performed by a spectrometer (av-400 MHz, Bruker) at 298 K. In the NMR measurement of Lewis acidic imidazolium chloroaluminate ILs, acetone- d_6 was used as an external standard to suppress the interference from other solvents [20]. All the peaks and corresponding chemical shifts obtained confirmed the structure and chemical composition of these ILs, and no impurity peaks were found in the NMR spectra.

The mass fraction of water in ILs was determined by Karl Fisher titration (751 GPD Titrino, Metrohm) [20]. For all the Lewis acidic chloroaluminate ILs, the results of measurement showed that the water content was below 50 ppm. The mass fraction purity of all the chloroaluminate ILs was determined to be >99.5%.

2.3. The measurement of physicochemical properties

An electrospray ionisation mass spectrometry (ESI-MS) (Micromass Q-TOF) was used to identify the structure of ions. The surface morphology and compositional analysis of aluminium deposits were examined with emission scanning electron microscope (SEM) (JSM-6700F, JEOL) and energy dispersive X-ray (EDAX) (XL30 S-FEG, FEI), respectively [20]. And the X-ray diffraction patterns (XRD) of aluminium deposits were determined on a X'Pert Pro MPD X-ray diffractometer (AXIOS, PANalytical) with Cu K α radiation ($\lambda = 0.15405$ nm). Dielectric constant of ILs was obtained by the network analyzer (E8362B, Agilent) according to previous literature [21]. The electrical conductivity, viscosity and density measurements were performed by conductivity meter (FE30, Mettler Toledo), automated microviscometer (AMVn, Anton Paar) and high-precision vibrating tube densimeter (DMA 5000, Anton Paar), respectively [17].

2.4. Electrochemical experiments

All the electrochemical experiments were conducted in the argon-filled glove box mentioned above. Experiments were performed with an electrochemical workstation (CHI660D, Shanghai Chenhua Instrument Co., Ltd.) controlled by CHI660D software in a three-electrode cell [20]. Pt plate working electrode (5×5 mm, Tianjin Aidahengchen Co., Ltd.) and Ptdisc counter electrode (3 mm radius, Tianjin Aidahengchen Co., Ltd.) were used in the electrochemical measurements. In all these experiments, the non-aqueous Ag⁺/Ag electrode (CHI112, Shanghai Chenhua Instrument Co., Ltd.) containing 0.01 M solution of AgNO₃ in [Bmim][NTf₂]/acetonitrile (298.2 K) was sealed and employed as reference electrode. Prior to use, all the working and counter electrodes were polished with emery paper, cleaned with acetone, treated with a dilute hydrochloric acid/sulfuric acid mixture and dried. All the ILs were heated in an oil bath and the accuracy of temperature was ±0.5 K (RET basic, IKA). After electrolysis experiments, the aluminium deposits were washed by absolute alcohol, deionized water and finally dried in air [20].

2.5. Computational methods

All the calculations for chloroaluminate ILs were conducted with the Gaussian09 program according to density functional theory (DFT). The geometries of all the studied ion pairs were optimized using Becke–three–parameter–Lee–Yang–Parr (B3LYP) with 6-31+G(d,p) basis set. Each optimized IL's structure has been checked to be a true minimum by frequency calculation at the corresponding level. Basis set superposition errors (BSSE) were considered for interaction energy through the counterpoise method [17].

3. RESULTS AND DISCUSSION

Considering the fact that predominant presence of anion in 1:2 [Rmim]Cl/AlCl₃ is [Al₂Cl₇][−] [14,17], all the chloroaluminate ILs are expressed by [Rmim][Al₂Cl₇] in the following text. Some basic physicochemical properties, such as viscosity, electrical conductivity and density of ILs are related to electrodeposition. Therefore, these properties have been measured and presented in Table 1. Obviously, ILs' structure, especially *N*-alkyl side chain has significant effect on above properties. According to our previous work, the difference in these properties is mainly attributed to different structural symmetry, interaction energy and hydrogen bonding between ions [17].

Table 1. The electrical conductivity κ , viscosity η and density ρ of ILs at 313.2 K

IL	κ	η	ρ
	mS/cm	mPa·s	g/cm ³
[H ₁ mim][Al ₂ Cl ₇]	9.61	23.28	1.476200
[Emim][Al ₂ Cl ₇]	20.61	11.47	1.378132
[Amim][Al ₂ Cl ₇]	16.16	14.95	1.346013
[Bmim][Al ₂ Cl ₇]	13.44	12.87	1.322868
[Hmim][Al ₂ Cl ₇]	12.36	16.80	1.278885

3.1. Surface morphology of aluminium deposits

The chemical composition and crystal structure of aluminium deposits have been confirmed by EDAX and XRD spectra (see Figure 1). The mass purity of all aluminium deposits was higher than 99.5%. To explore the surface morphology of aluminium deposits obtained from different chloroaluminate ILs, SEM measurements were carried out.

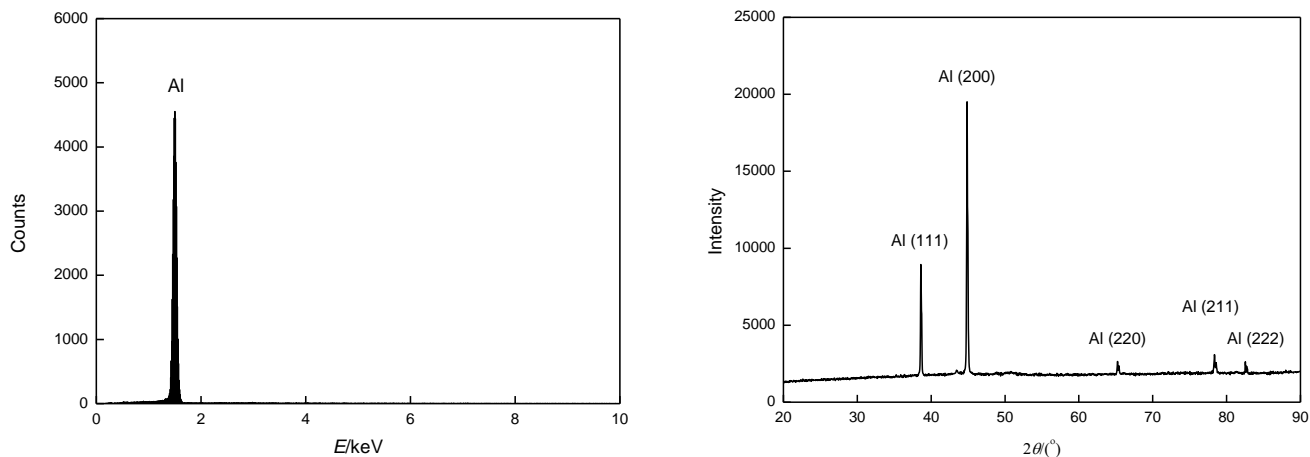


Figure 1. EDAX (left graph) and XRD spectra (right graph) of aluminium deposits obtained from Lewis acidic chloroaluminate ILs [Bmim][Al₂Cl₇] at 15 mA/cm² and 313.2 K.

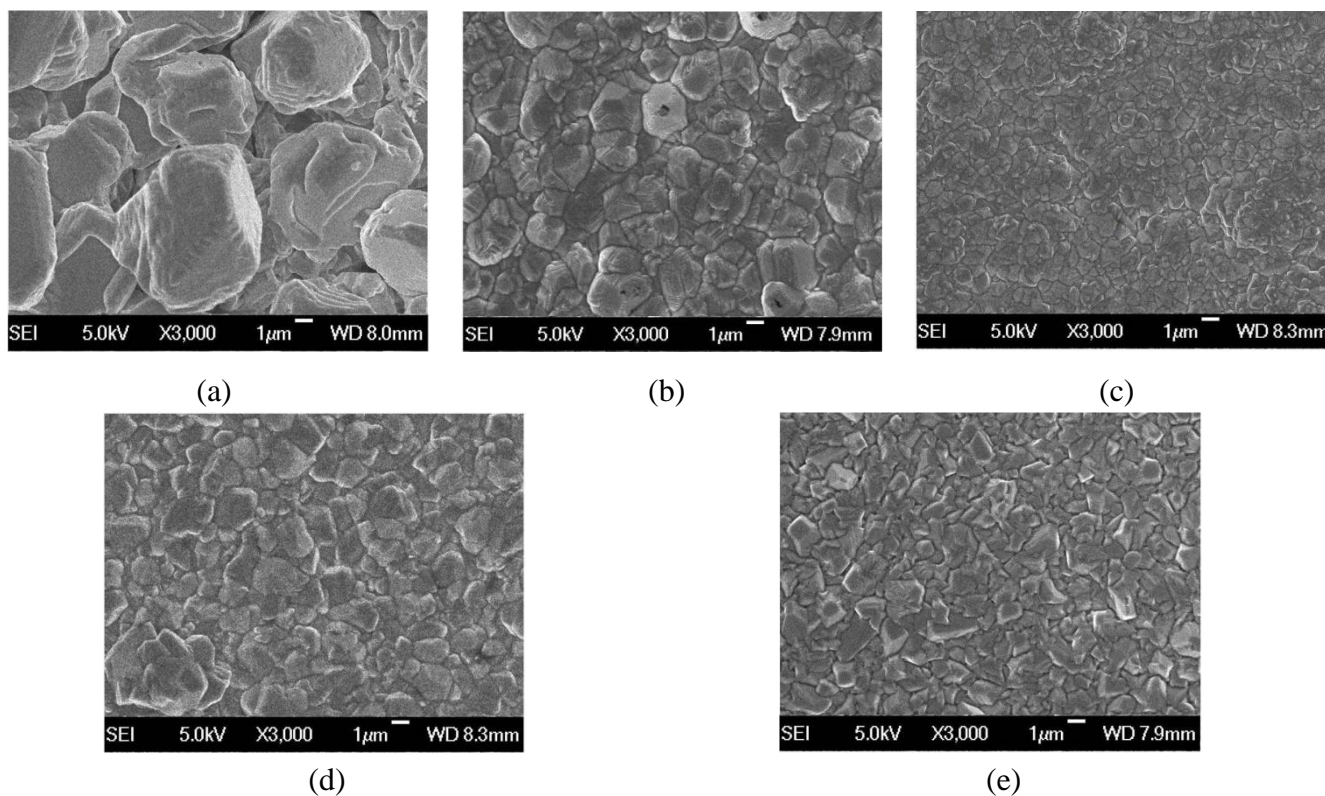


Figure 2. SEM micrographs of aluminium deposits obtained from Lewis acidic chloroaluminate ILs at 15 mA/cm² and 313.2 K. (a) [H₁mim][Al₂Cl₇]; (b) [Emim][Al₂Cl₇]; (c) [Amim][Al₂Cl₇]; (d) [Bmim][Al₂Cl₇]; (e) [Hmim][Al₂Cl₇].

Although all the chloroaluminate ILs are similar in molecular structure and chemical composition, research results shows that the resulting electrodeposits are quite different in shape and volume. As Figure 2 illustrates, the average grain size of aluminium crystallites deposited from these ILs follows the order, $[\text{H}_1\text{mim}][\text{Al}_2\text{Cl}_7]$ ($5\sim 8\ \mu\text{m}$) $>[\text{Emim}][\text{Al}_2\text{Cl}_7]$ ($3\sim 4\ \mu\text{m}$) $>[\text{Bmim}][\text{Al}_2\text{Cl}_7]$ ($2\sim 3\ \mu\text{m}$) $>[\text{Hmim}][\text{Al}_2\text{Cl}_7]$ ($1.5\sim 2\ \mu\text{m}$) $>[\text{Amim}][\text{Al}_2\text{Cl}_7]$ ($\sim 1\ \mu\text{m}$) at the same experimental conditions. It can be inferred that the difference in surface morphology of aluminium is probably attributed to structural variation of imidazolium cations and electrical double layer [14].

3.2. Results of electrochemical measurements

Based on above SEM micrographs, the difference in the surface morphology of deposits reflects that the growth of aluminium has experienced different electrochemical processes. Therefore, some electrochemical measurements, such as cyclic voltammetry, chronoamperometry and differential capacitance were performed to investigate corresponding reactions and electrical double layer in these chloroaluminate ILs.

3.2.1. Cyclic voltammetry

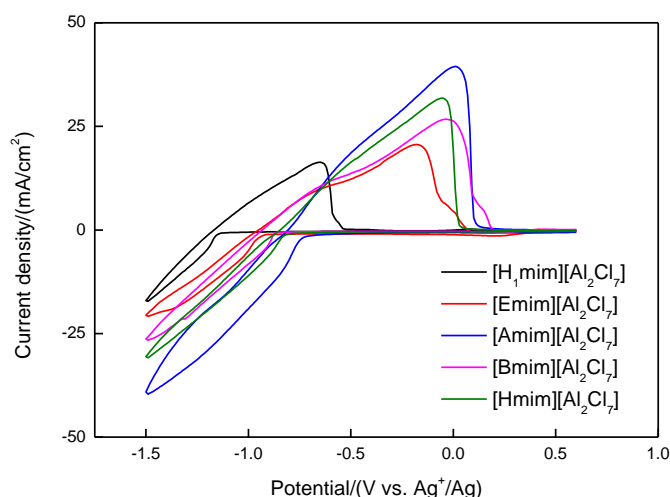


Figure 3. Cyclic voltammograms recorded on a Pt electrode in all the chloroaluminate ILs at 313.2 K (cathodic potential regime). The potential scan rate was 0.1 V/s.

As expected, a pair of reduction and oxidation peaks can be found in all the cyclic voltammograms. It reveals the electrodeposition and stripping process of aluminium on Pt electrode in chloroaluminate ILs (see Equation 1 and 2). However, the initial reduction potential V_{Re} of Al(III) in these electrolytes is quite different, increasing in the order $[\text{H}_1\text{mim}][\text{Al}_2\text{Cl}_7] < [\text{Emim}][\text{Al}_2\text{Cl}_7] < [\text{Bmim}][\text{Al}_2\text{Cl}_7] < [\text{Hmim}][\text{Al}_2\text{Cl}_7] < [\text{Amim}][\text{Al}_2\text{Cl}_7]$ at the same experimental conditions. In view of the relationship between applied potential and electrolytic reduction, it's proper to state that electrodeposition of aluminium is easier to conduct in the chloroaluminate ILs where corresponding initial potential of Al(III) is more positive [22]. For instance,

aluminium is more easily to be electrodeposited from [Bmim][Al₂Cl₇] than [H₁mim][Al₂Cl₇] at 313.2 K (see Figure 3). Higher current density is observed in [Bmim][Al₂Cl₇] at the same deposition potential.



3.2.2. Chronoamperometry

The surface morphology of aluminium deposits is highly depended on its nucleation and growth process. Thus, chronoamperometric measurement was used to evaluate the reaction mechanism in these chloroaluminate ILs [23]. The resulting current-time transients all display a classic shape for nucleation process, followed by current fluctuation of electrical double layer charging and crystal growth. As the applied deposition potential shifts more negative, the nucleation density rises and time needed for overlap of diffusion zones is shortened.

It's well-known that electrodeposition of aluminium on electrode always undergoes a three dimensional nucleation and growth process, which can be illustrated by instantaneous nucleation or progressive nucleation [24]. To identify the nucleation model of aluminium, the experimental time t and t_m (the time at current maximum) has been corrected for induction time t_0 before comparison. The time axis was redefined as $t' = t - t_0$ and $t'_m = t_m - t_0$ [25]. Figure 4 demonstrates the plots of $(i/i_m)^2$ vs. t'/t'_m which were obtained from the experimental data in chronoamperometric measurement. Apparently, electrodeposition of aluminium on Pt electrode is consistent with the three-dimensional instantaneous nucleation process in [H₁mim][Al₂Cl₇]. It indicates that all the nucleation sites for aluminium are activated at the outset of chronoamperometric experiments. Same conclusions have also been confirmed for aluminium electrodeposition in the other studied chloroaluminate ILs.

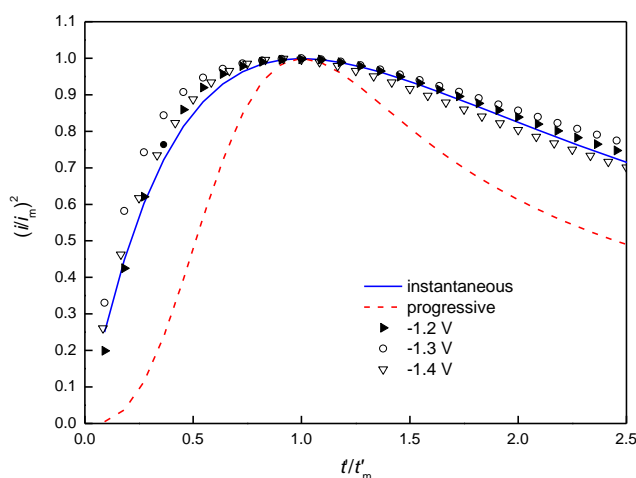


Figure 4. The dimensionless experimental current-time transients compared with theoretical curves for three-dimensional progressive and instantaneous nucleation mechanism on Pt electrode in [H₁mim][Al₂Cl₇] at 313.2 K.

3.2.3 Differential Capacitance

Based on above research and literature survey, it can be inferred that the structure of electrode/ions interface exerts a profound influence on electrochemical growth of aluminium [26]. Thus, differential capacitance measurement was performed to investigate the properties of electrical double layer between electrode surface and chloroaluminate ILs during deposition process.

To obtain the value of differential capacitance, impedance measurements were performed from scanning the potential from negative to positive direction. Based on experimental impedance data, the value of differential capacitance (C_d) was calculated by the following Equation 3, in which Z'' is the imaginary part of impedance (see Figure 5) [27]. Figure 6 shows the capacitance-potential curves recorded on a Pt electrode in all the chloroaluminate ILs within electrochemical windows. Obviously, all the curves display a typical camel shape as described for imidazolium ILs [28]. The local minimum in the curves is ascribed to potential of zero charge (PZC), at which there is no excess charge on Pt electrode interface. At the potential near PZC, counter ions generally accumulate around the surface of electrode. When applied potential shifts far away from PZC, the ions are hard to compensate for excess charge on electrode, resulting in decrease differential capacitance with potential.

$$-Z'' = \frac{1}{2\pi f C_d} \tag{3}$$

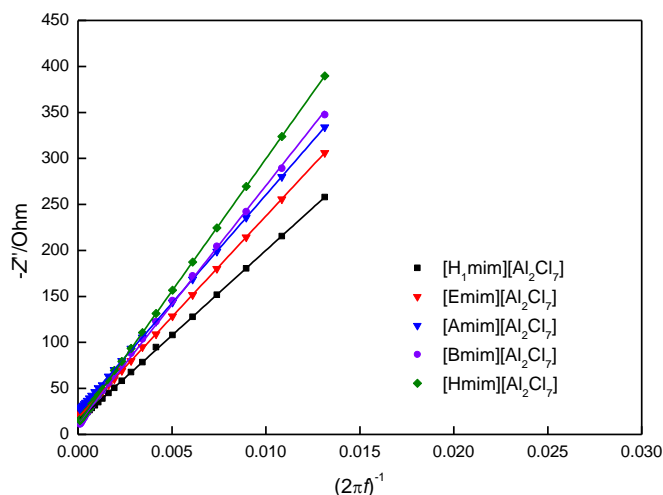


Figure 5. Nyquist plots for all the chloroaluminate ILs on Pt electrode at 313.2 K and PZC with wide frequency range.

A well-known model of electrified interface was proposed by Helmholtz, which can be expressed as Equation 4 illustrates. In this theoretical formula, ϵ , ϵ_0 and d stand for dielectric constant of materials (ILs), permittivity of free space and distance between capacitor plates, respectively [29]. On this basis, the value of d and relevant parameters of electrical double layer have been calculated and listed in Table 2.

$$C_d = \frac{\epsilon\epsilon_0}{d} \tag{4}$$

The value of PZC in these chloroaluminate ILs follows the order, $[H_1mim][Al_2Cl_7] < [Emim][Al_2Cl_7] < [Bmim][Al_2Cl_7] < [Hmim][Al_2Cl_7] < [Amim][Al_2Cl_7]$ at 313.2 K, which is in accordance with the order of initial reduction potential of Al(III). It implies that ions are more easily adsorbed onto Pt electrode if Al(III) is prone to be electrodeposited at the same potential. However, the parameter C_d of electrical double layer at PZC and density of ILs change in another trend as $[H_1mim][Al_2Cl_7] > [Emim][Al_2Cl_7] > [Amim][Al_2Cl_7] > [Bmim][Al_2Cl_7] > [Hmim][Al_2Cl_7]$ at 313.2 K. According to experimental results and literature survey [30], it can be inferred that the molecular properties of ILs, such as ionic volume, alkyl chain, polarizability and relative permittivity have important influence on the structure of electrical double layer.

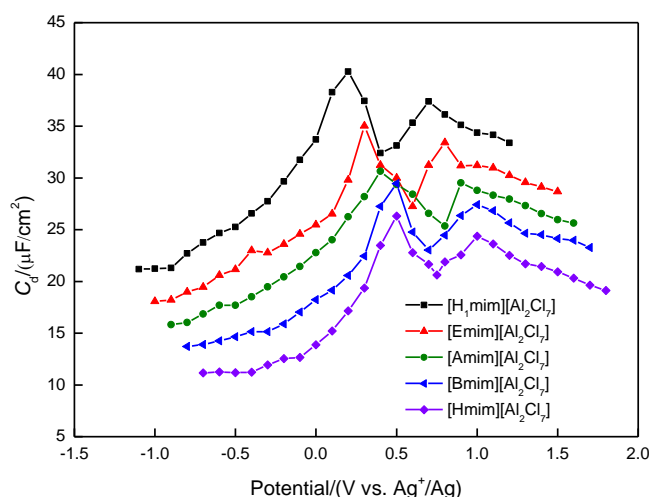


Figure 6. Capacitance-potential curves recorded on a Pt electrode in all the chloroaluminate ILs at 313.2 K.

Table 2. Parameters of electrical double layer at the electrode/ILs interface during aluminium electrodeposition at 313.2 K.

IL	V_{Re}	PZC	C_d	ϵ	d
	V	V	$\mu F/cm^2$	—	Å
$[H_1mim][Al_2Cl_7]$	-1.12	~0.40	32.41	12.95	3.54
$[Emim][Al_2Cl_7]$	-0.94	~0.60	27.25	13.66	4.44
$[Amim][Al_2Cl_7]$	-0.73	~0.80	25.36	13.93	4.86
$[Bmim][Al_2Cl_7]$	-0.86	~0.70	23.04	14.12	5.42
$[Hmim][Al_2Cl_7]$	-0.81	~0.75	20.63	14.28	6.13

3.3. Computational results

To gain more information on the properties of electrical double layer and ILs, theoretical calculations were performed by computational method. Figure 7 and Table 3 show the resulting optimized geometries and structural parameters of chloroaluminate ILs.

Interestingly, the dielectric constant ϵ , dipole moment μ , distance d (between capacitor plates) and diameter of imidazolium cation D all change in the same order $[\text{H}_1\text{mim}][\text{Al}_2\text{Cl}_7] < [\text{Emim}][\text{Al}_2\text{Cl}_7] < [\text{Amim}][\text{Al}_2\text{Cl}_7] < [\text{Bmim}][\text{Al}_2\text{Cl}_7] < [\text{Hmim}][\text{Al}_2\text{Cl}_7]$. It indicates that the increased length of alkyl chain on imidazolium cation enhances the dimensional asymmetry of ion-pairs. Meanwhile, the value of d is very close to that of D in the same chloroaluminate IL. These results reflect that the double layer formed at electrode interface is probably one-ion thick and can be seen as typical Helmholtz layer.

On the other hand, the interaction energy of ion pairs varies as $[\text{H}_1\text{mim}][\text{Al}_2\text{Cl}_7] > [\text{Emim}][\text{Al}_2\text{Cl}_7] > [\text{Bmim}][\text{Al}_2\text{Cl}_7] > [\text{Hmim}][\text{Al}_2\text{Cl}_7] > [\text{Amim}][\text{Al}_2\text{Cl}_7]$. Remarkably, this order is the same as that of V_{Re} , as well as the average grain size of aluminium deposits. Based on above experimental results and published work [14], it's proper to state that Al(III) is harder to be reduced in the chloroaluminate ILs with higher cation-anion interaction energy. Under such conditions, fewer nuclei are formed on the electrode during the three-dimensional instantaneous nucleation process, which usually leads to larger and rougher aluminium crystallites. Besides, it also proves that the Lewis acidic N -hydrogen atom in $[\text{H}_1\text{mim}][\text{Al}_2\text{Cl}_7]$ increases the cation-anion interaction energy and hydrogen bonding. By comparison, the introduction of double bond to N -alkyl side chain results in lower interaction energy among the ions of $[\text{Amim}][\text{Al}_2\text{Cl}_7]$.

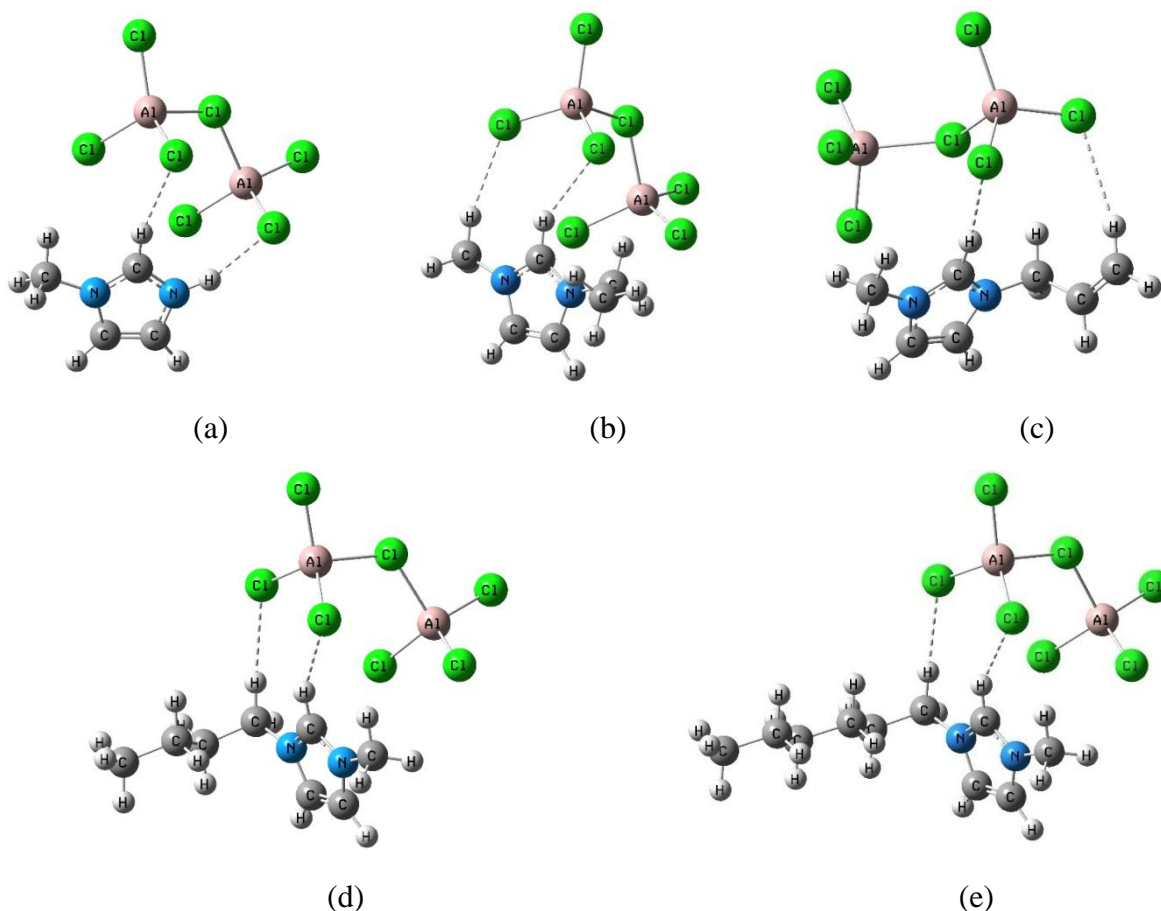


Figure 7. The optimized geometries of chloroaluminate ILs at B3LYP/6-31+G(d,p) level. Hydrogen bonds are illustrated by dashed lines. (a) $[\text{H}_1\text{mim}][\text{Al}_2\text{Cl}_7]$; (b) $[\text{Emim}][\text{Al}_2\text{Cl}_7]$; (c) $[\text{Amim}][\text{Al}_2\text{Cl}_7]$; (d) $[\text{Bmim}][\text{Al}_2\text{Cl}_7]$; (e) $[\text{Hmim}][\text{Al}_2\text{Cl}_7]$.

Table 3. Structural parameters of chloroaluminate ILs obtained by computational method.

IL	D^a	μ	E^b
	Å	Debye	kJ/mol
[H ₁ mim][Al ₂ Cl ₇]	3.73	14.25	295.90
[Emim][Al ₂ Cl ₇]	4.65	15.29	273.60
[Amim][Al ₂ Cl ₇]	5.04	15.44	261.84
[Bmim][Al ₂ Cl ₇]	5.69	15.56	270.61
[Hmim][Al ₂ Cl ₇]	6.58	15.65	268.96

^a calculated average diameter of imidazolium cation

^b the interaction energy of ion pairs

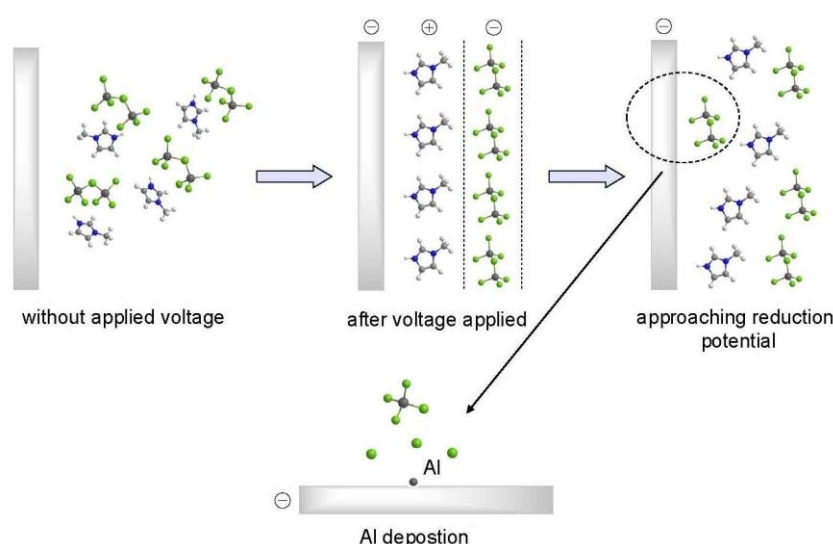


Figure 8. The proposed diagram of electrical double layer formation and aluminium electrodeposition on cathode.

On the basis of above discussion, it's proposed that the electrodeposition of aluminium on electrode can be divided into four main steps (see Figure 8). At first, there are mainly free ions adjacent to electrode. After voltage is applied, electrical double layer begins to form between ions and charging electrode interface. Accordingly, imidazolium cations are adsorbed onto cathode as the first layer. The second layer is composed of $[\text{Al}_2\text{Cl}_7]^-$ anions, which is less compact and associated with electrode. When it's close to the reduction potential of Al(III), some $[\text{Al}_2\text{Cl}_7]^-$ ions move toward cathode and pass through the first layer. Until reaching reduction potential, the Al(III) in $[\text{Al}_2\text{Cl}_7]^-$ is reduced into aluminium as nuclei. At last, more aluminium crystals are deposited on the nuclei, resulting in the final product.

In general, the interaction between ions plays an important role in aluminium electrodeposition. According to computational results, the introduction of Lewis acidic hydrogen atom to *N*-alkyl side chain can enhance the interaction between ions. By contrast, the presence of Lewis basic double bond in side chain (allyl group) weakens the interaction. It's demonstrated that the strength of cation-anion

interaction strongly depends on the electrostatic force between imidazolium cation and $[\text{Al}_2\text{Cl}_7]^-$ anion. The structure of *N*-alkyl side chain, especially functional group has great effect on the value of interaction energy. As interaction energy increases, $[\text{Al}_2\text{Cl}_7]^-$ is more difficult to be dissociated, penetrate the electrical double layer and approach the electrode surface. Thus, it impedes the effective reduction of $[\text{Al}_2\text{Cl}_7]^-$ and following aluminium deposition in chloroaluminate ILs, which always results in lower nucleation density and larger microcrystalline aluminium. Although ILs' electrical conductivity, viscosity and density may influence the mass and charge transfer of ions, it proves that the cation-anion interaction energy has greater impact on electrodeposition process, especially surface morphology of aluminium.

4. CONCLUSIONS

In present study, a series of classic imidazolium chloroaluminate ILs were used as low-temperature electrolytes. SEM micrographs show that the structure of electrical double layer between ILs and electrode has significant influence on surface morphology of resulting aluminium deposits. According to electrochemical measurements, initial reduction potential of Al(III) follows the order, $[\text{H}_1\text{mim}][\text{Al}_2\text{Cl}_7]^- < [\text{Emim}][\text{Al}_2\text{Cl}_7]^- < [\text{Bmim}][\text{Al}_2\text{Cl}_7]^- < [\text{Hmim}][\text{Al}_2\text{Cl}_7]^- < [\text{Amim}][\text{Al}_2\text{Cl}_7]^-$ at the same experimental conditions. Meanwhile, all the electrodeposition of aluminium is consistent with three-dimensional instantaneous nucleation process. However, the results of electrical double layer capacitance are quite different in these ILs. Based on computational methods, it can be concluded that the interaction between cations and anions is key to electrodeposition process. The introduction of Lewis acidic hydrogen atom to *N*-alkyl side chain can enhance interaction between ions. By contrast, the presence of Lewis basic double bond in side chain weakens the interaction. The value of interaction energy is highly affected by the structure of *N*-alkyl side chain, especially functional group. As the interaction energy of ions increases, $[\text{Al}_2\text{Cl}_7]^-$ is more difficult to penetrate the double layer and be reduced at electrode surface, which always results in larger grain size and rougher aluminium deposits. Therefore, interaction energy should be adjusted to a lower value by regulating the structure of imidazolium cation, in order to achieve finer and smoother aluminium crystals. It's hoped that this work could provide deeper insight into the electrodeposition behavior of aluminium in chloroaluminate ILs.

In future work, it's necessary to improve the molecular structure and electrochemical properties of chloroaluminate ILs. More *in situ* measurements, such as scanning probe microscopy and atomic force microscopy should be conducted in the exploration of double layer at electrode/ion interface. For the industrial application of technology, we also have to establish systemic regulation mechanism of aluminium deposition with further experiments.

ACKNOWLEDGEMENTS

This work was supported by the National Natural Science Foundation of China (No. 21406002, U1404217), the Science & Technology Development Program of Anyang and the Doctor Starting Foundation of Anyang Institute of Technology.

References

1. D. Pradhan, D. Mantha and R. G. Reddy, *Electrochim. Acta*, 54 (2009) 6661
2. D. Pradhan and R. G. Reddy, *Metall. Mater. Trans. B*, 43B (2012) 519
3. T. Rodopoulos, L. Smith, M. D. Horne and T. R  ther, *Chem. Eur. J.*, 16 (2010) 3815
4. Q. H. Zhang and J. M. Shreeve, *Chem. Rev.*, 114 (2014) 10527
5. M. V. Fedorov and A. A. Kornyshev, *Chem. Rev.*, 114 (2014) 2978
6. J. Park, C. K. Lee, K. Kwon and H. Kim, *Int. J. Electrochem. Sci.*, 8 (2013) 4206
7. G. K. Yue, S. J. Zhang, Y. L. Zhu, X. M. Lu, S. C. Li and Z. X. Li, *AIChE J.*, 55 (2009) 783
8. A. Bakkar and V. Neubert, *Electrochem. Commun.*, 51 (2015) 113
9. P. Giridhar, S. Zein El Abedin and F. Endres, *Electrochim. Acta*, 70 (2012) 210
10. A. Bakkar and V. Neubert, *Electrochim. Acta*, 103 (2013) 211
11. S. Zein El Abedin, P. Giridhar, P. Schwab and F. Endres, *Electrochem. Commun.*, 12 (2010) 1084
12. P. F. Sheng, B. Chen, H. B. Shao, J. M. Wang, J. Q. Zhang and C. N. Cao, *Mater. Corros.*, 66 (2015) 1338
13. Y. Z. Su, Y. C. Fu, Y. M. Wei, J. W. Yan and B. W. Mao, *ChemPhysChem*, 11 (2010) 2764
14. A. P. Abbott, F. Qiu, H. M. A. Abood, M. R. Ali and K. S. Ryder, *Phys. Chem. Chem. Phys.*, 12 (2010) 1862
15. R. Atkin, S. Zein El Abedin, R. Hayes, L. H. S. Gasparotto, N. Borisenko and F. Endres, *J. Phys. Chem. C*, 113 (2009) 13266
16. H. Ohno and M. Yoshizawa, *Solid State Ionics*, 154/155 (2002) 303
17. Y. Zheng, K. Dong, Q. Wang, J. M. Zhang and X. M. Lu, *J. Chem. Eng. Data*, 58 (2013) 32
18. Y. Zheng, X. P. Xuan, J. J. Wang and M. H. Fan, *J. Phys. Chem. A*, 114 (2010) 3926
19. J. G. Huddleston, A. E. Visser, W. M. Reichert, H. D. Willauer, G. A. Broker and R. D. Rogers, *Green Chem.*, 3 (2001) 156
20. Y. Zheng, C. H. Peng, Y. J. Zheng, D. Y. Tian and Y. Zuo, *Int. J. Electrochem. Sci.*, 11 (2016) 6095
21. M. M. Huang, Y. Jiang, P. Sasisanker, G. W. Driver and H. Weing  rtner, *J. Chem. Eng. Data*, 56 (2011) 1494
22. S. Schaltin, M. Ganapathi, K. Binnemans and J. Fransaer, *J. Electrochem. Soc.*, 158 (2011) D634
23. M. Zhang, J. S. Watson, R. M. Counce, P. C. Trulove and T. A. Zawodzinski Jr, *J. Electrochem. Soc.*, 161 (2014) D163
24. J. J. Lee, B. Miller, X. Shi, R. Kalish and K. A. Wheeler, *J. Electrochem. Soc.*, 147 (2000) 3370
25. T. Jiang, M. J. Chollier Brym, G. Dub  , A. Lasia and G. M. Brisard, *Surf. Coat. Technol.*, 201 (2006)1
26. F. Endres, O. H  fft, N. Borisenko, L. H. Gasparotto, A. Prowald, R. Al-Salman, T. Carstens, R. Atkin, A. Bund and S. Zein El Abedin, *Phys. Chem. Chem. Phys.*, 12 (2010) 1724
27. M. T. Alam, M. M. Islam, T. Okajima and T. Ohsaka, *Electrochem. Commun.*, 9 (2007) 2370
28. V. Lockett, R. Sedev, J. Ralston, M. Horne and T. Rodopoulos, *J. Phys. Chem. C*, 112 (2008) 7486
29. S. Baldelli, *J. Phys. Chem. B*, 109 (2005) 13049
30. V. Lockett, M. Horne, R. Sedev, T. Rodopoulos and J. Ralston, *Phys. Chem. Chem. Phys.*, 12 (2010) 12499